



LAWRENCE  
LIVERMORE  
NATIONAL  
LABORATORY

# Progress towards materials science above 1000 GPa (10 Mbar) on the NIF laser

B. A. Remington, H.-S. Park, S. T. Prisbrey, S. M. Pollaine, R. M. Cavallo, R. E. Rudd, K. T. Lorenz, R. Becker, J. Bernier, N. Barton, T. Arsenlis, S. G. Glendinning, A. Hamza, D. Swift, A. Jankowski, M. A. Meyers

March 26, 2009

9th International Conference on the Mechanical and Physical Behaviour of Materials under Dynamic Loading  
Brussels, Belgium  
September 7, 2009 through September 11, 2009

## **Disclaimer**

---

This document was prepared as an account of work sponsored by an agency of the United States government. Neither the United States government nor Lawrence Livermore National Security, LLC, nor any of their employees makes any warranty, expressed or implied, or assumes any legal liability or responsibility for the accuracy, completeness, or usefulness of any information, apparatus, product, or process disclosed, or represents that its use would not infringe privately owned rights. Reference herein to any specific commercial product, process, or service by trade name, trademark, manufacturer, or otherwise does not necessarily constitute or imply its endorsement, recommendation, or favoring by the United States government or Lawrence Livermore National Security, LLC. The views and opinions of authors expressed herein do not necessarily state or reflect those of the United States government or Lawrence Livermore National Security, LLC, and shall not be used for advertising or product endorsement purposes.

Progress towards materials science above 1000 GPa (10 Mbar) on the NIF laser\*

B.A. Remington,<sup>a</sup> H.-S. Park,<sup>a</sup> S.T. Prisbrey,<sup>a</sup> S.M. Pollaine,<sup>a</sup> R.M. Cavallo,<sup>a</sup> R.E. Rudd,<sup>a</sup>  
K.T. Lorenz,<sup>a</sup> R. Becker,<sup>a</sup> J. Bernier,<sup>a</sup> N. Barton,<sup>a</sup> T. Arsenlis,<sup>a</sup> S.G. Glendinning, A.  
Hamza,<sup>a</sup> D. Swift, A. Jankowski,<sup>b</sup> M.A. Meyers<sup>c</sup>

<sup>a</sup>)Lawrence Livermore National Laboratory, Livermore, CA;

<sup>b</sup>)Texas Technological University, Lubbock, TX;

<sup>c</sup>)University of California - San Diego, CA

Paper for the DYMAT-2009 Conference  
Brussels, Belgium  
7-11 Sept. 2009

**Abstract**

Solid state dynamics experiments at extreme pressures,  $P > 1000$  GPa (10 Mbar), and ultrahigh strain rates ( $1.e6-1.e8$  1/s) are being developed for the National Ignition Facility (NIF) laser. These experiments will open up exploration of new regimes of materials science at an order of magnitude higher pressures than have been possible to date. Such extreme, solid state conditions can be accessed with a ramped pressure drive. The experimental, computational, and theoretical techniques are being developed and tested on the Omega laser. Velocity interferometer measurements (VISAR) establish the high pressure conditions generated by the ramped drive. Constitutive models for solid state strength under these conditions are tested by comparing simulations with experiments measuring perturbation growth from the Rayleigh–Taylor instability in solid state samples of vanadium. Radiography techniques using synchronized bursts of x-rays have been developed to diagnose this perturbation growth. Experiments on Omega demonstrating these techniques at peak pressures of  $\sim 1$  Mbar will be discussed. The time resolved observation of foil cracking and void formation show the need for tamped samples and a planar drive. \*This work performed under the auspices of the U.S. Department of Energy by Lawrence Livermore National Laboratory under Contract DE-AC52-07NA27344.

**I. INTRODUCTION**

With the advent of modern high energy, high power, pulsed laser systems, such as the Omega and NIF lasers, the ability to study solid-state material dynamics at ultrahigh pressures and ultrahigh strain rates has become possible. On the Omega lasers, designs for ramped pressures  $> 1$  Mbar have been achieved, [Lorenz, 2006] and on NIF, ramped pressures  $> 10$  Mbar have been developed. [Remington, 2009; Park, 2008] In the experiments to be discussed here, the high power Omega laser is focused at an intensity of  $I_L \sim 2.5 \times 10^{13}$  W/cm<sup>2</sup> for 3.7 ns onto a 200  $\mu$ m thick, layered plastic reservoir corresponding to layers of polyimide, CH, and CH(2%Br), glued together. This launches a strong shock through the reservoir that breaks out the back, and unloads (decompresses as a plasma) across a 300  $\mu$ m vacuum gap to stagnate against the vanadium sample, as illustrated in the upper inset in Fig. 1. [Edwards, 2004] The 35  $\mu$ m thick sputtered

polycrystalline V samples are thermally insulated from the heat in this stagnated reservoir plasma by a  $\sim 7 \mu\text{m}$  thick epoxy heat shield, which is machined flat on the gap side. The grain sizes ranged from 0.5-2  $\mu\text{m}$  in the lateral direction, longer in the foil thickness direction, with aspect ratio of 3-5 (see lower inset in Fig. 1). The resulting pressure vs time is deduced from a series of drive shots, using a VISAR diagnostic to measure the loading vs. time on surrogate Al-LiF samples (10  $\mu\text{m}$  Al, 500  $\mu\text{m}$  LiF). [Lorenz, 2006] The resulting pressure vs time for the vanadium RT samples to be discussed here is shown in Fig. 1. [Park, 2009] Peak pressures of  $\sim 1$  Mbar are reached at  $t = 28\text{-}33$  ns (where  $t = 0$  corresponds to when the laser first turns on), with loading on the sample commencing at  $\sim 24$  ns, loading rise time of  $\sim 4\text{-}5$  ns, high pressure FWHM of  $\sim 11$  ns, and a slow decay, falling below 100 kbar at  $t > 60$  ns. This causes a peak acceleration in the vanadium sample of  $\sim 0.7 \mu\text{m}/\text{ns}^2 = 7 \times 10^{13} \text{ cm}/\text{s}^2 = (7 \times 10^{10})g_0$ , where  $g_0$  is the acceleration due to gravity at the surface of the earth. It is this acceleration that triggers the RT growth at the rippled interface. The overall time scales of these experiments (10-100 ns) are short, but the accelerations are high. Hence, significant solid-state deformation dynamics can occur over these very short time scales.

The vanadium samples were created with a sinusoidal ripple of wavelength of  $\lambda = 60 \mu\text{m}$ , amplitude of 0.6  $\mu\text{m}$  (ie, half the peak-to-valley height) on one surface. The rippled surface is then coated with  $\sim 7 \mu\text{m}$  of epoxy, called the heat shield, which is machined flat on its free surface. When the shock unloaded reservoir stagnates against the epoxy heat shield, the pressure rises to  $\sim 1$  Mbar, which accelerates the vanadium whose back side is a free surface (no tamper). Upon acceleration, the rippled epoxy-vanadium interface is hydrodynamically unstable due to the Rayleigh-Taylor (RT) instability. The amplitude of the ripple tends to grow in size (the ripple wavelength remains unchanged). In the absence of material strength in the vanadium, this ripple amplitude would grow very rapidly due to the RT instability. Material strength at high pressures (0.1 - 1 Mbar) and very high strain rates ( $10^6\text{-}10^7 \text{ s}^{-1}$ ) generates a very strong stabilizing force. The net result is that the rate and magnitude of RT-induced perturbation amplitude growth is greatly reduced. The degree to which the RT growth is decreased (from what it would have been in the absence of strength) is a measure of the strength. [Lorenz, 2005] The higher the strength, the lower the RT growth. For example, in the absence of material strength, the amplitude of the ripple would have grown by factors of 50-100, whereas in the actual experiments, growth factors of 10-15 were observed. The details of these V-RT measurements, and comparisons with material strength models, are described elsewhere. [Park, 2009]

In this paper, we will focus on observations that occurred at later times,  $t \geq 100$  ns (compared to times near peak pressure, which occurs at  $\sim 30$  ns), in the V-RT experiments. We will discuss in this paper observations of dynamic crack initiation and growth during high strain rate deformation ( $\text{few} \times 10^7 \text{ s}^{-1}$ ) of vanadium. In Fig. 2 we show a sequence of 2D face-on gated x-ray radiographs taken using timed bursts of 5.2 keV  $\text{He}_\alpha$  x-rays. The rippled growth due to the RT instability is observed as enhanced contrast of optical depth modulation ( $\Delta\text{OD}$ ), with lighter regions corresponding to thinner regions of vanadium (RT "bubbles"), and darker regions corresponding to thicker regions of vanadium (RT "spikes"). The modulation in optical depth can approximately be

written as  $\Delta OD \sim \Delta(\kappa \rho z) \sim \kappa \Delta(\rho z) \sim \kappa \rho_{av} \Delta z$ , where  $\kappa \sim 100 \text{ cm}^2/\text{g}$  is the opacity of vanadium at 5.2 keV. Hence, knowing the opacity and average density (from the known equation of state - EOS), the average spatial modulation can be inferred. The modulation amplitude is growing in time due to the RT instability.

Figure 2 shows gated 2D radiographs from a sequence of individual laser shots at nominally the same drive conditions. The grain size of the V used in Figs. 2a-2f corresponds to  $\sim 0.6 \text{ }\mu\text{m}$  in the lateral direction. The perturbation amplitude grows with time up to a peak growth factor (rippled final amplitude / initial amplitude) of 10-14 at  $t = 70 \text{ ns}$  (Figs. 2a-2c). By 100 ns, the ripple character has started to change (Fig. 2d). The lighter regions (ripple valleys) now show regions of localized 3D thinning, which we interpret as voids opening up in the thinnest regions of the valleys. By 130 ns, it appears that these voids have coalesced into cracks running the full extent of the ripple valleys (Fig. 2e). We show a similar image in Fig. 2f corresponding to a somewhat lower peak pressure experiment ( $P_{\text{max}} \sim 600 \text{ kbar}$ ), at a time of 140 ns. Here again, the ripple valleys have formed cracks along the full extent of the driven region of the foil. There is an interesting mottled texture in the darker regions (RT "spikes") suggesting these regions of vanadium between the cracks are starting to break up or fragment into 3D pieces of size 20-30  $\mu\text{m}$ .

Figures 2g and 2h show an even more dramatic result. In this case, the V foils were prepared with 3x larger grains (lateral size of  $\sim 1.8 \text{ }\mu\text{m}$ ). This corresponds to a reduced ambient strength by a factor of  $\sim 1.6$  (460 MPa vs 715 MPa), in reasonable agreement with the Hall-Petch effect. In this case, now very dramatic void growth is observed along the rippled valleys earlier in time at 55 ns (Fig. 2g), which are starting to coalesce along the valleys. This represents an observation of the evolution of incipient crack formation at ultrahigh strain rates,  $d\epsilon/dt \sim \text{few} \times 10^7 \text{ s}^{-1}$ , with nanosecond time resolution at spatial resolution of  $\sim 15 \text{ }\mu\text{m}$  (see Fig. 2h). We believe this is an experimental first.

To understand these dynamics, we first did 2D radiation-hydrodynamics simulations using the code LASNEX [Zimmerman, 1975]. From this, we simulated the foil 2D evolution, including pressure, density, temperature, and strain vs time. During the first  $\sim 40 \text{ ns}$ , these simulations were validated with VISAR measurements, which lead to the pressure vs time curve shown in Fig. 1. During the first  $\sim 40 \text{ ns}$ , the foil shape is still reasonably planar (Fig. 3a). Late in time,  $t > 50 \text{ ns}$ , the simulations show that the foil exhibits very distinct bowing, evolving towards a hemispherical shape, as shown in Fig. 3b. The experimental 2D radiographs also show the evolution towards a hemispherical shape, as the ripples near the periphery appear to be close together than those at the center of the driven region. This observation can easily be converted into an experimental measure of the degree of bowing, as shown by the red circles and thick red arc in Fig. 3b. The agreement between the measured shape and simulated shape is very good, giving us confidence in our understanding of the overall foil evolution.

The validated drive from the LASNEX simulations was then used as input to the ALE3D code, including a new multiscale material strength model, [Bernier, 2009], to calculate the rippled growth and other details of the ripple evolution. The results from a 2D run

from ALE3D is shown in Fig. 4 at 66 ns, where we show 2D color plots of density (4a), pressure (4b), temperature (4c), strain (4d), and strain rate (4e). By this late time of 66 ns, the peak pressure has dropped to just under 100 kbar, the peak strain is  $\sim 1.2$ , ie, greater than 100%, and the strain rates are very high, in the range of  $10\text{-}30\ \mu\text{s}^{-1} = 1\text{-}3 \times 10^7\ \text{s}^{-1}$ . A key observation from the simulations comes from looking closely at the conditions on the free surface side at the thinnest regions (ripple valleys). Figure 4a shows the back side of the ripple valley is underdense, dropping slightly below the ambient density. The corresponding pressure (Fig. 4b) at the back of the ripple valley is negative, at -11 kbar. At 30 ns, this negative pressure was as high as -18 kbar, whose magnitude is 2.5x larger than the ambient yield strength for this material of 7.2 kbar. It seems very likely, due to this negative pressure under the rippled valleys, that voids grow from the back surface, which are observed as the localized 3D thin regions in the valleys at late time. Further, the overall strain at failure,  $\sim 100\%$ , at these strain rates is 1-2 orders of magnitude larger than value determined from bench tensile tests. From bench tensile measurements of these same grain sizes,  $\epsilon_{\text{failure}} \sim 0.01$  and  $0.09$  for the onset of failure for the 0.6mm and 1.6mm grain material resp. These voids are observed much earlier in time for the lower strength, larger grain material, where the negative pressure is  $\sim 4\text{x}$  larger (in magnitude) than the ambient yield strength of 4.60 kbar. When these voids grow and link up in the RT ripple valleys, a crack is formed. We believe this is the first experimental observations of incipient crack formation at ultrahigh strain rates ( $\sim 10^7\ \text{s}^{-1}$ ), with nanosecond time resolution.

## REFERENCES

- [Bernier, 2009] J. Bernier et al., Nat. Mat., to be submitted (2009).
- [Edwards, 2004] J. Edwards et al., PRL 92, 075002 (2004).
- [Lorenz, 2005] K.T. Lorenz et al. Phys. Plasmas 12, 056309 (2005).
- [Lorenz, 2006] K.T. Lorenz et al. HEDP 2, 113 (2006).
- [Park, 2008] H.S. Park et al., J. of Physics: Conf. Ser. 112, 042024 (2008).
- [Park, 2009] H.S. Park et al., PRL, to be submitted (2009).
- [Remington, 2008] B.A. Remington et al., MST 22, 474 (2008).
- [Remington, 2009] B.A. Remington et al., submitted, HEDP (Dec. 2008).
- [Zimmerman, 1975] G.B. Zimmerman and W.L. Kruer, Com. Plasma Phys. Control. Fusion 2, 51 (1975).

## FIGURE CAPTIONS

Figure 1. Pressure vs. time at the front face of the vanadium sample. Upper inset shows an illustration of how the ramped drive works. Lower inset shows an optical image of a cross section of the smaller grained V; the average lateral grain size was  $\sim 0.6\ \mu\text{m}$ .

Figure 2. Sequence of 2D gated x-ray images of V-RT foils as they evolve. (a) - (e) correspond to a  $\sim 1$  Mbar maximum pressure drive, whereas (f) represents a 600 kbar maximum pressure drive. (g) and (h) had  $1.6\ \mu\text{m}$  lateral grain sizes, whereas all the rest had the smaller  $0.6\ \mu\text{m}$  lateral grain size. The grains were elongated by factors of 3-5 in the foil thickness direction.

Figure 3. 2D LASNEX simulations showing 2D isodensity contours of the foil gross evolution at (a) 40 ns and (b) 130 ns. The red plotting symbols and thick red curve in (b) corresponds to experimental measurements of the foil bowing, normalized to the location of the simulation at the vertex of the quasi-hemisphere.

Figure 4. 2D plots of (a) density, (b) pressure, (c) temperature, (d) strain, and (e) strain rate at 66 ns, using the code ALE-3D.

"  
"

Vj ku'y qtnlr gthqto gf 'wpf gt'yj g'cwur legu'qh'yj g'WUOF gr ctvo gpv'qh'Gpgti { 'd{ 'Ncy tgpeg"  
Nlxgto qtg"P cvkqpcnNcdqtcvqt { 'wpf gt'EqpvcevfF G/CE74/29P C495660

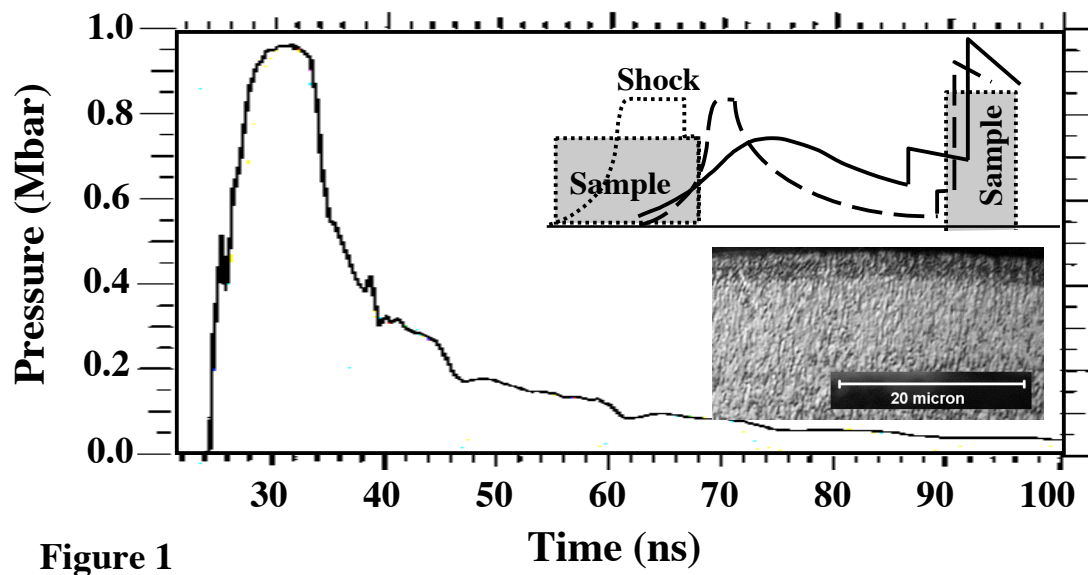


Figure 1

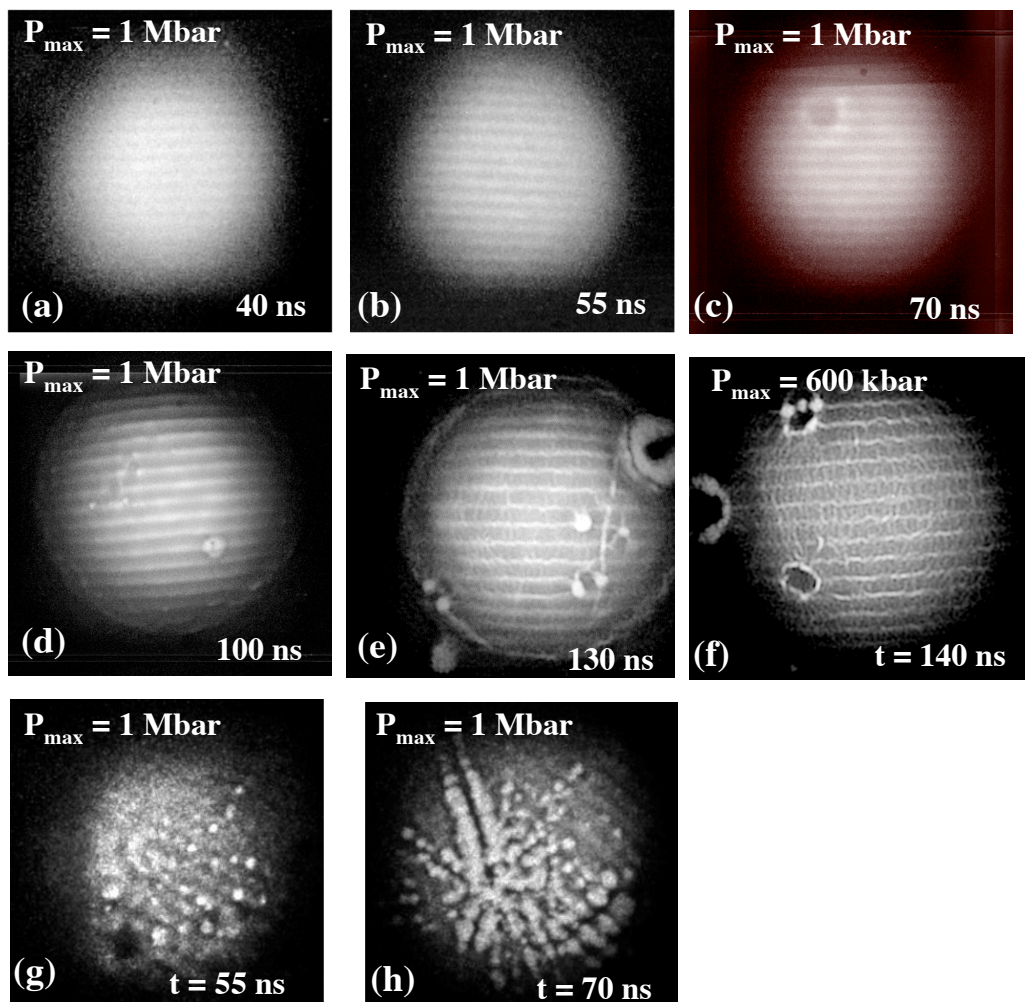


Figure 2



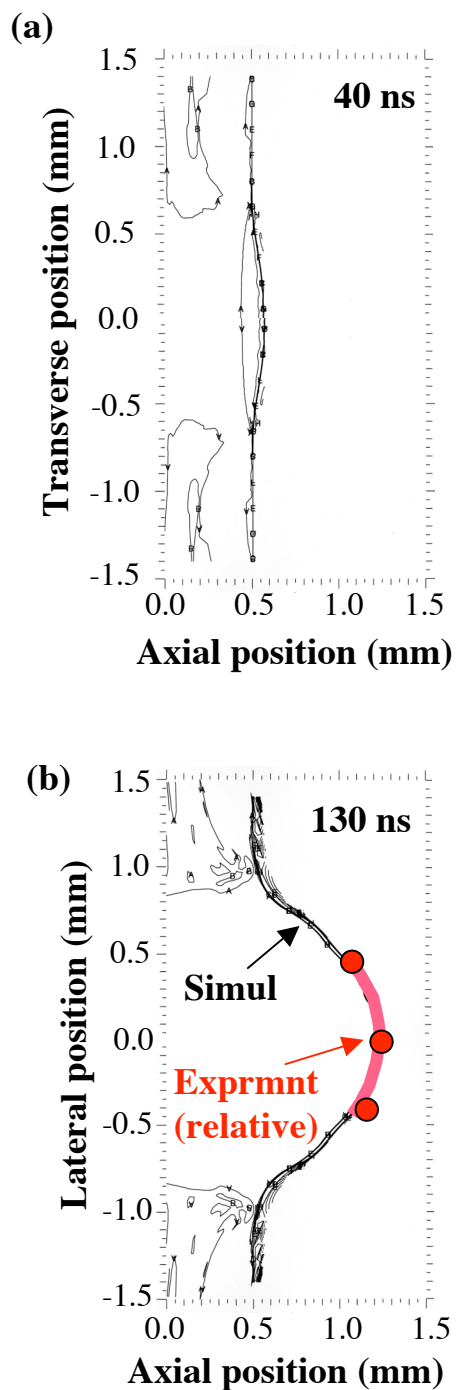


Figure 3

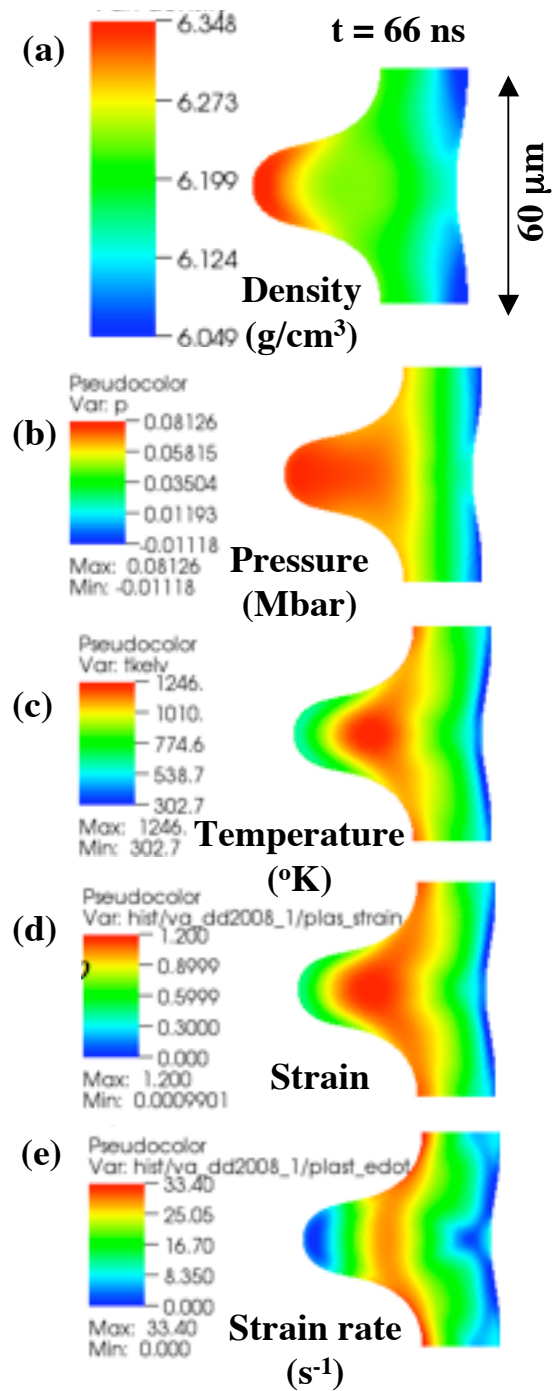


Figure 4